

An ancestral HIV-2/simian immunodeficiency virus peptide with potent HIV-1 and HIV-2 fusion inhibitor activity

Pedro Borrego^{a,b}, Rita Calado^{a,b}, José M. Marcelino^c,
Patrícia Pereira^{b,d}, Alexandre Quintas^{a,b},
Helena Barroso^{a,b} and Nuno Taveira^{a,b}

Objectives: To produce new fusion inhibitor peptides for HIV-1 and HIV-2 based on ancestral envelope sequences.

Methods: HIV-2/simian immunodeficiency virus (SIV) ancestral transmembrane protein sequences were reconstructed and ancestral peptides were derived from the helical region 2 (HR2). The activity of one ancestral peptide (named P3) was examined against a panel of HIV-1 and HIV-2 primary isolates in TZM-bl cells and peripheral blood mononuclear cells and compared to T-20. Peptide secondary structure was analyzed by circular dichroism. Resistant viruses were selected and resistance mutations were identified by sequencing the *env* gene.

Results: P3 has 34 residues and overlaps the N-terminal pocket-binding region and heptad repeat core of HR2. In contrast to T-20, P3 forms a typical α -helical structure in solution, binds strongly to the transmembrane protein, and potently inhibits both HIV-2 (mean IC₅₀, 63.8 nmol/l) and HIV-1 (11 nmol/l) infection, including T-20-resistant isolates. The N43K mutation in the HR1 region of HIV-1 leads to 120-fold resistance to P3 indicating that the HR1 region in transmembrane glycoprotein is the target of P3. No HIV-2-resistant mutations could be selected by P3 suggesting that the genetic barrier to resistance is higher in HIV-2 than in HIV-1. HIV-1-infected patients presented significantly lower P3-specific antibody reactivity compared to T-20.

Conclusion: P3 is an HIV-2/SIV ancestral peptide with low antigenicity, high stability, and potent activity against both HIV-1, including variants resistant to T-20, and HIV-2. Similar evolutionary biology strategies should be explored to enhance the production of antiviral peptide drugs, microbicides, and vaccines.

© 2013 Wolters Kluwer Health | Lippincott Williams & Wilkins

AIDS 2013, **27**:000–000

Keywords: ancestral P3 peptide, inhibition of HIV-1 and HIV-2 cell fusion and entry, P3 antigenic reactivity, P3 mechanism of action, resistance to P3

Introduction

Over the last decade, the inhibition of viral entry has become one of the most attractive fields in the research for

new anti-HIV-1 molecules. Currently, there are two entry inhibitors approved for antiretroviral therapy, the fusion inhibitor peptide enfuvirtide (or T-20; Fuzeon; Roche) [1] and the CCR5 antagonist maraviroc

AQ1

^aUnidade dos Retrovírus e Infecções Associadas, Centro de Patogénese Molecular (URIA-CPM), Faculdade de Farmácia da Universidade de Lisboa, Avenida das Forças Armadas, Lisbon, ^bCentro de Investigação Interdisciplinar Egas Moniz (CiiEM), Instituto Superior de Ciências da Saúde Egas Moniz, Quinta da Granja Monte de Caparica, Caparica, ^cUnidade de Microbiologia Médica, Instituto de Higiene e Medicina Tropical, Universidade Nova de Lisboa (IHMT, UNL), and ^dResearch Institute for Medicines and Pharmaceutical Sciences (iMed.UL), Faculdade de Farmácia da Universidade de Lisboa, Avenida Prof. Gama Pinto, Lisbon, Portugal.

Correspondence to Nuno Taveira, PharmD, PhD, Unidade dos Retrovírus e Infecções Associadas, Centro de Patogénese Molecular, Faculdade de Farmácia da Universidade de Lisboa, Avenida das Forças Armadas, 1649–019 Lisbon, Portugal.

Tel: +351 21 793 4212; fax: +351 21 793 4212; e-mail: ntaveira@ff.ul.pt

Received: 30 January 2012; revised: 22 December 2012; accepted: 10 January 2013.

DOI:10.1097/QAD.0b013e32835edc1d

(Selzentry; Pfizer) [2]. T-20 is a linear peptide composed of 36 amino acids that mimics the sequence of gp41 helical region 2 (HR2) of the HIV-1 LAI isolate [3,4]. T-20 inhibits HIV-1 entry by competitive binding to the complementary helical region 1 (HR1), thereby blocking the formation of the six-helix bundle structure and preventing viral fusion [5–7]. Despite strong anti-HIV-1 activity, the genetic barrier for T-20 resistance is low [7,8] and resistance mutations are usually found within the 36–45 positions of HR1 region [7,9]. T-20 has poor bioavailability and has to be injected subcutaneously twice daily, complicating patient adherence to treatment. Currently, T-20 is only used as a salvage therapy in HIV-1 infection [10–12]. Novel fusion inhibitor peptides have been developed in an attempt to improve antiviral potency, increase in-vivo stability, and overcome T-20 resistance [7,13]. T-1249 is a representative second generation 39-mer peptide derived from HR2 consensus sequences [14,15]. It is a strong inhibitor of HIV-1 but the elevated production costs and drug formulation difficulties associated with its long size, have hampered its clinical development beyond phase I/II trials [16]. Sifuvirtide is a third generation fusion inhibitor peptide that has shown promising results in phase II clinical studies being active against a broad range of HIV-1 isolates, including T-20-resistant strains [7,13,17].

HIV type 2 (HIV-2), the second causative agent of AIDS, is responsible for localized epidemics mainly in west Africa and in few other countries (e.g., Portugal and France), affecting an estimated 1–2 million patients worldwide [18]. HIV-2 is composed of eight groups termed A–H of which group A is by far the most disseminated worldwide [19–21]. HIV-1 and HIV-2 have different evolutionary histories [22] and share only 50% of genetic similarity [23]. Consequently, some anti-HIV-1 drugs have limited or no activity on HIV-2, namely nonnucleoside reverse transcriptase inhibitors, some protease inhibitors, and T-20 [4,24,25]. T-20 has no activity on HIV-2 possibly because its sequence divergence from HIV-2 prevents it from binding to the HR1 target in gp36 envelope glycoprotein [24,26,27]. The aim of the current work was to produce new HR2-based peptides to inhibit HIV-2 fusion and entry. To enhance the likelihood of inhibiting replication of all HIV-2 strains, the candidate peptides were derived from ancestral HIV-2 and SIVmn gp36 sequences. We found that one selected peptide, named P3, potently inhibited the fusion and entry of both HIV-1 and HIV-2.

Materials and methods

Virus stocks and titration

A total of 26 primary isolates were included in this study (seven HIV-1 and 19 HIV-2); all isolates were characterized for coreceptor usage as described previously

[27]. HIV reference strains were obtained by transfection of HEK293T cells with pNL4-3 (HIV-1), pSG3.1 (HIV-1), or pROD10 (HIV-2) plasmids using Fugene 6 reagent (Roche, Switzerland) according to manufacturer's instructions. Pseudoviruses carrying the vesicular stomatitis virus (VSV) envelope were produced by cotransfection of HEK293T cells with pSG3.1 Δ env plasmid and a plasmid expressing VSV envelope (pHEF-VSVG). HIV-1 variants resistant to T-20 were propagated in CEM-SS cells according to a protocol available at www.aidsreagent.org. The 50% tissue culture infectious dose (TCID₅₀) of all viruses was determined in a single-round viral infectivity assay using a luciferase reporter gene assay in TZM-bl cells [27].

Peptide design

Custom peptides were derived from ancestral gp36 HR2 sequences reconstructed from a phylogenetic tree of HIV-2 and simian immunodeficiency virus (SIV) reference sequences (see Support Digital Content 1, <http://links.lww.com/QAD/A306> for a list of reference sequences used). Reconstruction of ancestral character states was performed by maximum likelihood in PAUP version 4 software [28]. MODELTEST [29] estimated best-fit models of molecular evolution for maximum likelihood analyses. The chosen model was GTR+G+I [30]. Tree searches were also performed in PAUP version 4.0 using the nearest-neighbor interchange (NNI) and tree bisection and reconnection (TBR) heuristic search strategies and bootstrap resampling.

Peptides were produced commercially by Genemed Synthesis (San Antonio, Texas, USA). They were modified with the N-terminus acetylated and the C-terminus as a carboxamide, the salt form being acetate. Reverse-phase high-pressure liquid chromatography (HPLC) was used for purification (>95%) and mass spectrometry for confirmation analysis.

Circular dichroism spectroscopy

Circular dichroism spectra were recorded for P3 and T-20 in 10 mmol/l phosphate buffer and 100 mmol/l NaF (pH 7.4) using a Jasco 810 spectropolarimeter equipped with a temperature control unit Julabo F25. Spectra were recorded at 25°C in the far ultraviolet (UV) region (185–240 nm), using a 0.1 cm pathlength cell (Helma UL, Lda), with a 50 nm/s scan speed, an 8-s response time, and 2 nm bandwidth. For each spectrum, four scans were averaged. P3 and T-20 concentration was previously determined by absorbance at 280 nm using an extinction coefficient of $\epsilon_{280} = 13940 \text{ M}^{-1} \text{ cm}^{-1}$ and $\epsilon_{280} = 18350 \text{ M}^{-1} \text{ cm}^{-1}$, respectively, in a UV-Visible spectrophotometer Jasco V-530. The final concentration used for P3 and T-20 was of 104 and 47 $\mu\text{mol/l}$, respectively. For protein secondary structure estimation, circular dichroism spectra were deconvoluted using the CDSSTR [31] deconvolution algorithm on Dichroweb [32,33]. Circular dichroism

AQ2

limited

AQ3

spectra of the appropriate buffers were recorded and subtracted from the protein spectra.

Peptide-binding assay

An ELISA assay

ELISA was developed to study the binding specificity of peptide P3 to its predicted target in HIV-2 *env* gp36. Polystyrene immune module microwells (Maxisorp; Nunc, Roskilde, Denmark) were coated with each peptide at a concentration of 50 $\mu\text{g}/\text{ml}$ in phosphate buffered saline (PBS) solution and incubated overnight at 4°C. After two washes with PBS, microwells were blocked with 5% of bovine serum albumin (BSA; Sigma-Aldrich, USA) in PBS for 2 h at 37°C and washed twice with PBS. A recombinant gp36 protein with a polyhistidine tag (rgp36) previously produced in our laboratory [34] was diluted in PBS containing 0.05% of Tween-20 (Bio-Rad, USA) (PBS-T) and added (100 μl) at a concentration of 2.5 $\mu\text{g}/\text{ml}$ and incubated for 1 h at 37°C. After five washes with PBS-T, a 1 : 2000 dilution of mouse monoclonal antipolyhistidine antibody conjugated to alkaline phosphatase (Sigma-Aldrich) in PBS-T was added (100 μl) and incubated for 1 h at 37°C. After another five washes with PBS-T, p-nitrophenyl phosphate tablets (Sigma-Aldrich) were added as a chromogenic substrate, and the optical density was measured in a Tecan MP-500 plate reader (Tecan, Männedorf, Switzerland) at 405 nm against a reference wavelength of 620 nm. The cut-off value of the assay, calculated as the mean optical density value of negative controls + two times the standard deviation (SD), was determined for each peptide using wells in which the peptide was incubated with PBS instead of rgp36. The results of the assay are expressed quantitatively as optical density_{peptide}/optical density_{cut-off} ratios (optical density/cut-off ratio).

AQ4

AQ5

Drug susceptibility assays

The antiviral activity of fusion inhibitors was evaluated using a single-round viral infectivity assay and a viral replication inhibition assay. The former was performed using the TZM-bl reporter cells as previously described [27]. Briefly, cells were infected with 200 TCID₅₀ of each virus. Infections were performed in the presence of serial-fold dilutions of inhibitors in growth medium, supplemented with DEAE-dextran. After 48 h of infection, luciferase expression was quantified with the One-Glow luciferase assay substrate reagent (Promega, USA) according to manufacturer's instructions. The cytotoxicity of the compounds was evaluated using control wells in the absence of the virus. Additional cell viability studies were also performed in peripheral blood mononuclear cells (PBMCs) incubated in the presence of up to 20 $\mu\text{mol}/\text{l}$ of peptide and evaluated with alamarBlue reagent (Invitrogen, USA).

For the viral replication inhibition assay, phytohemagglutinin-stimulated PBMCs were infected at a multiplicity of infection of 0.01 in the presence of serial-fold dilutions of inhibitors in growth medium, followed by incubation for 7–11 days. Viral replication was measured

by a p24 assay (INNOTEST HIV Antigen mAb; Innogenetics, Ghent, Belgium).

At least two independent experiments were performed for each analysis and each assay was set up in duplicate wells. Dose–response curve parameters were estimated using the sigmoidal dose–response (variable slope) equation in Prism version 4.0c for Macintosh (GraphPad Software, San Diego, California USA, www.graphpad.com).

Time-of-addition experiments

Time-of-addition experiments were set in single-round viral infectivity assays to measure the antiviral activity of P3 against HIV-1 (strain SG3.1) and HIV-2 (strain ROD) at different time-points. T-20 and AMD3100 were used as controls for inhibiting different stages of viral entry. TZM-bl cells were infected with 200 TCID₅₀ of HIV-1SG3.1 in the presence of P3 (129 nmol/l), T-20 (1 nmol/l), or AMD3100 (58 nmol/l) or with 200 TCID₅₀ of HIV-2ROD in the presence of P3 (876 nmol/l) or AMD3100 (32 nmol/l). These concentrations correspond to two-fold the IC₉₀ value of each drug [27]. The peptide was added at various times either before or after infection. In the former, the peptide was added both to cells and viruses in separate. When added to cells only, an additional washing step with PBS (twice with 200 μl) was performed before proceeding to infection. Luciferase expression was quantified after 48 h of infection as mentioned above.

Antigenic reactivity assay

A new ELISA assay was developed to measure antigenic reactivity of peptides in HIV-infected patients using an ELISA protocol similar to the one described for the binding assay. Briefly, microwells were independently coated with each peptide at a concentration of 10 $\mu\text{l}/\text{ml}$ in PBS solution and incubated overnight at 4°C. After blocking with BSA, 100 μl of a 1 : 300 dilution of plasma samples collected from 29 HIV-2 and 30 HIV-1-infected patients (all naive to T-20) in PBS-T was added and incubated for 1 h at 37°C. Wells were then washed six times with PBS containing 0.1% of Tween 20 and a 1 : 2000 dilution of goat antihuman immunoglobulin G (Fc specific) conjugated to alkaline phosphatase (Sigma-Aldrich) in PBS-T was added. Following incubation, the color was developed and optical densities were measured as described above. The clinical cut-off value of the assay, calculated as the mean optical density value of HIV-seronegative samples + two times the SD, was determined using samples from healthy HIV-seronegative individuals ($n = 10$). The results of the assay are expressed quantitatively as optical density_{clinical sample}/optical density_{cut-off} ratios (optical density/cut-off ratio).

Selection of P3 resistance mutations

Primary HIV-1 and HIV-2 strains were used for selection of resistance mutations to P3 in PBMCs, using a standardized procedure as described elsewhere [35].

Phytohemagglutinin-stimulated PBMCs were infected at a multiplicity of infection of 0.01 and selections started with concentrations below the IC_{50} level. Viral replication was monitored weekly by p24 antigen assay. Culture supernatants were harvested for subsequent genotypic analysis by sequencing. To this end, RNA was extracted using QIAmp viral RNA Mini Kit (Qiagen, Germany), according to manufacturer's instructions, and reverse transcribed using Titan One Tube RT-PCR System (Roche, Switzerland). The *env* gene (positions 6203–8817 in HIV-1 HXB2 and positions 6673–9268 in HIV-2 BEN) was amplified by nested PCR, with the Expand Long Template PCR System kit (Roche, Switzerland) and sequenced. Primers used for amplification and sequencing are described in Support Digital Content 2 and 3, <http://links.lww.com/QAD/A306>.

Statistical analysis

Statistical analyses were performed using Prism version 4.0c for Macintosh (GraphPad Software) with a level of significance of 5%.

Results

Design and structure of ancestral peptides

Maximum likelihood methods were used to reconstruct ancestral transmembrane protein sequences at several nodes of the envelope gene phylogenies that represent ancestors to diverse HIV and SIV virus clades (Fig. 1a). These sequences were aligned (Fig. 1b) and three peptides were derived covering different functional domains of the HR2: P1 (36 mer), P2 (42 mer), and P3 (34 mer) (Fig. 1c). Due to high hydrophobicity, P1 and P2 were very difficult to synthesize and reconstitute in an appropriate buffer suitable for cell culture assays. Therefore, only P3 was analyzed for antiviral activity. P3 overlaps the N-terminal pocket-binding region and heptad repeat core of the HR2 region (positions 628–661 of HIV-1 HXB2 Env). It differs by 21 amino acids from the consensus HIV-1 sequence and by six amino acids from consensus HIV-2. However, the positions *a* and *d* of the heptad repeat, considered critical for HIV-1 HR1/HR2 binding [36], were quite conserved. There were only four changes: I635V and Y638L, involving amino

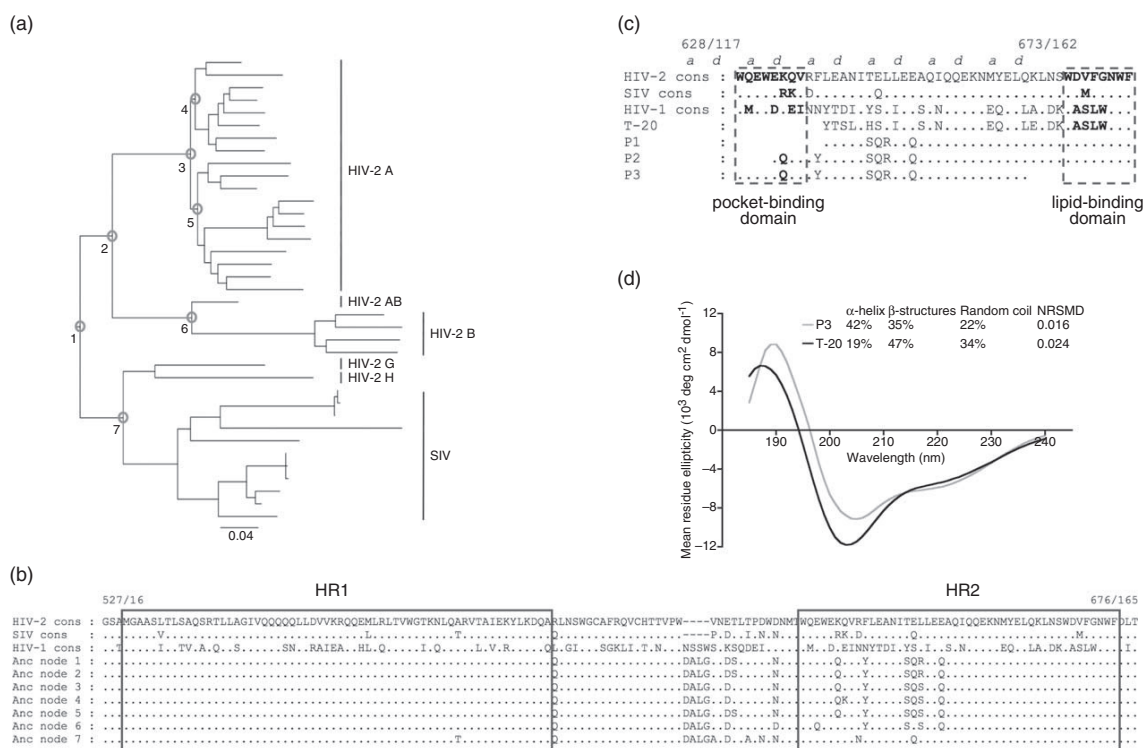


Fig. 1. Sequence and structure of ancestral peptides. (a) Ancestral reconstruction of HIV-2 gp36 sequences; the interior nodes highlighted by numbered circles in the phylogenetic tree correspond to the ancestral sequence used for peptide design. The scale bar represents evolutionary distances in substitutions per site. (b) Alignment of the gp41/gp36 HR1-HR2 segment, containing HIV-2, simian immunodeficiency virus (SIV), and HIV-1 consensus sequences, as well as the ancestral sequences. Points represent similarity relative to HIV-2 consensus and dashes represent gaps in the alignment. Sequences are numbered according to HIV-1 HXB2, Env position/gp41 position. (c) Alignment of consensus HR2 sequences from HIV-2, SIV, and HIV-1 with T-20, P1, P2, and P3. Sequences are numbered according to HIV-1 HXB2, Env position/gp41 position. Positions *a* and *d* of HR2 represent the residues involved in HIV-1 HR1/HR2 interaction. The pocket-binding domain and lipid-binding domains are highlighted. (d) Circular dichroism spectra for P3 and T-20 peptides. β -structures include sheets and turns. NRSMD, normalized root mean square deviation.

acids with hydrophobic side chains, and L645R and S649A, involving amino acids from different chemical groups.

T-20 and P3 overlap in 24 amino acids of the heptad repeat core and diverge in 14 residues (58%). P3 is more hydrophilic than T-20 (percentage of hydrophilic residues is of 62% in P3 and 56% in T-20) [37] and its predominant secondary structure in solution is an α -helix (42%). T-20 has a lower content of regular secondary structure elements in solution with only 19% of helicity, as previously reported (Fig. 1d) [38].

P3 is a potent inhibitor of HIV-1 and HIV-2 infection

The antiviral activity of peptide P3 was first evaluated in single-round viral infectivity assays against 20 group A HIV-2 isolates, of which 19 were primary isolates, and nine HIV-1 isolates, including seven highly diverse primary isolates (Support Digital Content 4, <http://links.lww.com/QAD/A306>). P3 potently inhibited both HIV-2 and HIV-1 infection (Table 1). Remarkably, P3 was significantly more active against HIV-1 than against HIV-2 (IC_{50} were 63.8 nmol/l for HIV-2 vs. 11 nmol/l for HIV-1, $P < 0.0001$). Similar results were obtained in the viral replication inhibition assay in PBMCs. P3 inhibited HIV-2 and HIV-1 replication in PBMCs at IC_{50} of 109.3 and 12.1 nmol/l, respectively ($P < 0.0001$; Support Digital Content 5, <http://links.lww.com/QAD/A306>). No cytotoxicity was observed *in vitro* either in TZM-bl culture cells or primary PBMCs at all concentrations tested (up to 20 μ mol/l). P3 did not inhibit the entry of a pseudovirus carrying the vesicular stomatitis virus envelope glycoprotein (VSV-G) indicating that its antiviral activity is HIV-envelope specific (Support Digital Content 6, <http://links.lww.com/QAD/A306>).

Compared with T-20, P3 was significantly more active as judged by the IC_{50} against HIV-2 and significantly less active against HIV-1 ($P < 0.0001$ for both cases; Table 1 and Fig. 2). Nonetheless, P3 and T-20 had similar IC_{90} ranges (P3, 6.2–1785.5 nmol/l; T-20, 0.5–

1285.3 nmol/l) and similar dose–response curve slopes when tested against HIV-1, predicting similar antiviral activity *in vivo* [39,40]. Importantly, the antiviral activity of P3 and T-20 was null after washing cells that were preexposed to these peptides with PBS (Fig. 3a). In contrast, AMD3100 remained fully active. P3 lost almost 30% of its activity when added 3 h after virus infection but sustained its potent activity even when added 3 h prior to infection. In all, these results indicate that P3 is quite stable and that it inhibits viral fusion by binding to the virus particles and not to the cell.

P3 and T-20 bound strongly to rgp36, a recombinant HIV-2 transmembrane protein in an ELISA assay (30-fold above the cut-off for P3; Fig. 3b). This suggested that the activity of P3, like that of T-20 and other fusion inhibitor peptides, was mediated through strong binding to its putative target in the transmembrane glycoprotein of the envelope complex [41]. To investigate the binding activity of these peptides to HIV-1, we expressed the rgp41 polypeptide equivalent to the rgp36 polypeptide. However, neither P3 nor T-20 bound to rgp41 in the ELISA assay (data not shown) suggesting that unlike rgp36, rgp41 does not form the coiled-coil structure to which T-20 (and most likely P3) bind in the virus particles [42]. Why rgp41 does not assume this coiled-coil structure and rgp36 apparently does is unknown at this time.

The antigenicity of P3 and T-20 peptides was examined with plasma samples collected from HIV-2-infected and HIV-1-infected patients, all naive to T-20. The majority of HIV-2 patients (93%) had P3-specific antibodies, whereas 45% had T-20-specific antibodies (data not shown). This was expected as the amino acid sequence of P3 was derived from an ancestral HIV-2/SIV sequence. Likewise, the majority of HIV-1 patients (90%) had T-20-specific antibodies, whereas 67% had P3-specific antibodies. Of note, the mean binding affinity of the T-20-specific antibodies from HIV-1 patients was significantly higher compared to P3-specific antibodies (Fig. 3c). These results demonstrate that P3 is weakly antigenic in HIV-1 patients compared to T-20.

Table 1. Antiviral activity of P3 and T-20 against HIV-1 and HIV-2 primary isolates.

Parameter ^a	P3 (nmol/l)	T-20 (nmol/l) ^b	<i>P</i> value ^c
HIV-1 (<i>n</i> = 9)			
IC ₅₀ (95% CI)	11 (6.5–18.4)	1.2 (0.7–2.2)	<0.0001
IC ₉₀ (95% CI)	366.4 (117.5–1145.5)	95.9 (26.3–350.8)	0.107
Hill slope (95% CI)	0.6 (0.4–0.82)	0.5 (0.4–0.6)	0.263
HIV-2 (<i>n</i> = 20)			
IC ₅₀ (95% CI)	63.8 (51.9–78.5)	281.5 (223.2–354.9)	<0.0001
IC ₉₀ (95% CI)	709.6 (435.5–1158.8)	3881.5 (2393.3–6280.6)	<0.0001
Hill slope (95% CI)	0.9 (0.7–1.1)	0.8 (0.7–1)	0.492

^aIC₅₀, IC₉₀, and Hill slope best-fit values were inferred from sigmoidal dose–response (variable slope) curves adjusted to combined results of HIV-1 and HIV-2 isolates, and represent geometric mean values; 95% CI – 95% confidence interval.

^bT-20 susceptibilities were obtained for the same HIV-1 and HIV-2 viral panel [27].

^c*P* value for comparison of best-fit values using the *F*-test.

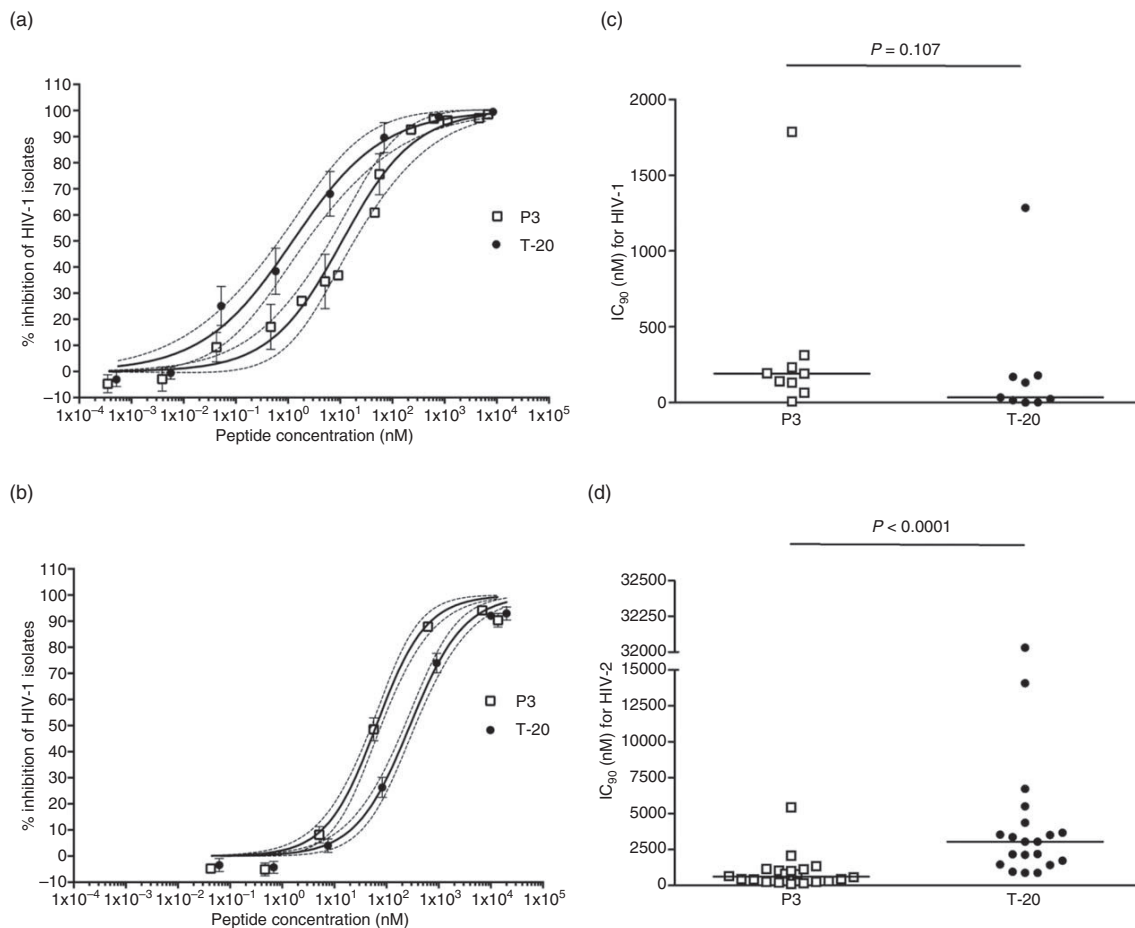


Fig. 2. Antiviral activity of P3. Representative dose–response curves for HIV-1 (a) and HIV-2 (b) with P3 and, for comparison, T-20 [27]. Data points represent the average of results obtained for HIV-1 ($N = 9$) and HIV-2 ($N = 20$) primary isolates; bars represent standard error of the mean. Sigmoidal dose–response (variable slope) curves were adjusted to these data points; dashed lines represent the 95% confidence band of the best-fit curve. Mean IC_{90} values of P3 and T-20, for HIV-1 (c) and HIV-2 (d) primary isolates. Bars represent median values. P values were obtained comparing best-fit values inferred from sigmoidal dose–response (variable slope) curves using the F -test.

P3 inhibits the replication of most T-20-resistant HIV-1 variants

To determine whether P3 is able to inhibit the infection of HIV-1 strains resistant to T-20, we measured the susceptibility of HIV-1 variants carrying well defined T-20 resistance mutations to P3 [43,44]. Notably, P3 exhibited potent activity against all but one T-20-resistant strains (IC_{50} range, 0.15–11.8 nmol/l; Table 2). The mutation N43K conferred high-level resistance to both P3 (2140-fold) and T-20 (2677-fold). Moreover, the V38A/N42D mutations conferred increased susceptibility to P3 (seven-fold lower IC_{50} compared to the wild-type). These results suggest that P3 could be used as an alternative for the treatment of patients infected with T-20-resistant HIV-1 strains.

Selection of P3-resistant variants

To investigate the mechanism of action and the pathways of resistance to P3, resistance mutations were selected

in vitro by repeated passage of HIV-1 and HIV-2 primary isolates in PBMCs in the presence of either constant or increasing concentrations of P3, according to the viral replication capability [35]. For HIV-1, the N43K substitution in the HR1 region of gp41 was the only mutation selected in *env* after 59 days in culture (eight passages) in the presence of 212 nmol/l of P3. Inhibition of replication of this mutant virus with P3 occurred at an IC_{50} of 1.9 μ mol/l and IC_{90} of 13.1 μ mol/l, which represent a 120-fold and 56.4-fold decrease in susceptibility, respectively. Under the same experimental conditions and despite repeated attempts, we were not able to select P3-resistant HIV-2 isolates. Collectively, these results indicate that the HR1 region in the transmembrane glycoprotein is the target of P3 and suggest that the pathway of HIV-1 resistance to P3 differs from that of T-20 and the genetic barrier to P3 resistance is significantly higher in HIV-2 than in HIV-1.

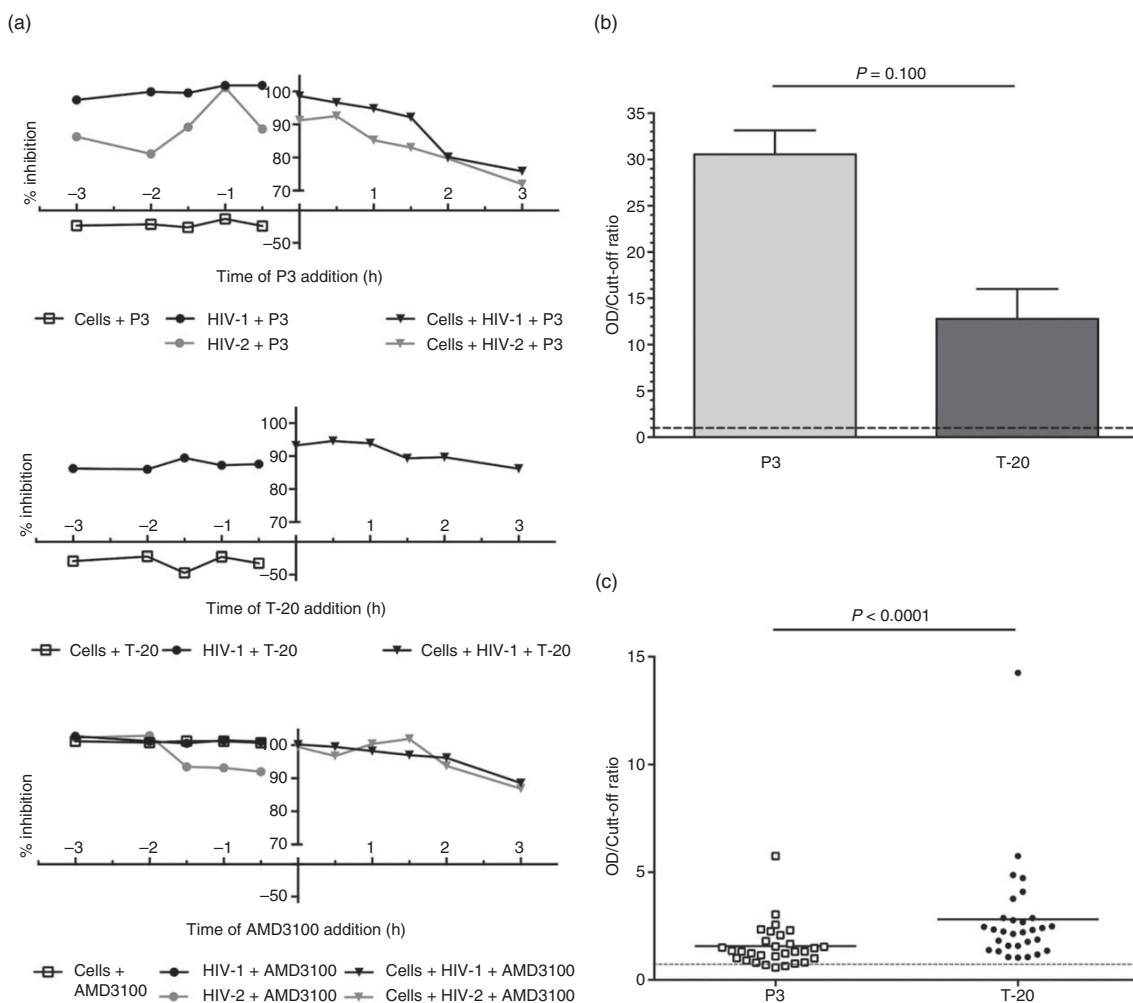


Fig. 3. Mechanism of action and antibody reactivity of P3. (a) Time-of-addition assays for P3 with HIV-1 and HIV-2. T-20 and AMD3100 were used as control drugs. In these experiments, each drug was added at different time-points either before (cells and viruses, separately) or after HIV infection. (b) Binding activity of P3 and T-20 to HIV-2 rgp36 in an ELISA assay. (c) Antibody reactivity of P3 and T-20 in HIV-1-infected patients. Bars represent mean values. Results from P3 are in open squares and from T-20 are in closed circles. *P* values were obtained with the Mann–Whitney *U*-test.

Table 2. Comparison of antiviral activity of P3 and T-20 on T-20-resistant HIV-1 variants.

HIV-1 variant	Susceptibility to T-20 ^a	P3		T-20		<i>P</i> value ^c
		IC ₅₀ nmol/l (95% CI)	Fold-increase ^b	IC ₅₀ nmol/l (95% CI)	Fold-increase ^b	
NL4-3 D36G (parental)	S	0.4 (0.2–1.2)	1	0.03 (0.01–0.06)	1	0.0002
NL4-3 (D36G) V38A	R	1.5 (0.5–5.1)	3.8	43.8 (21.8–87.8)	1460	<0.0001
NL4-3 (D36G) V38A/N42D	R	0.06 (0.01–0.3)	0.15	118.2 (63.0–221.7)	3940	<0.0001
NL4-3 (D36G) V38A/N42T	R	4.7 (1.9–11.5)	11.8	482.0 (324.1–716.8)	16 066.7	<0.0001
NL4-3 (D36G) N42T/N43K	R	855.9 (628.0–1167.0)	2139.8	80.3 (61.1–105.6)	2676.7	<0.0001

CI, confidence interval.

^aSensitive (S) or Resistant (R).

^bFold-increase of IC₅₀ concentration relative to NL4-3 D36G (parental).

^c*P* value for comparison of best-fit values between P3 and T-20, using the *F*-test.

Discussion

We show here that an ancestral peptide (named P3) derived from the HR2 domains of HIV-2 and SIV transmembrane glycoproteins potently inhibits both HIV-1 and HIV-2 cell entry and replication. The rationale for using ancestral sequences of the transmembrane envelope glycoprotein as a source for the new antiviral peptide was to minimize HIV sequence divergence by tracing the most likely evolutionary path along the phylogeny and capture more conserved structural features of the HR2 sequences [45,46]. The potent activity of P3 against divergent HIV-1 and HIV-2 primary isolates demonstrates that our strategy was highly successful. The potent activity of P3 on HIV-1 was not expected but it might be due to the conservation in P3 of the residues located in critical positions involved in the HR1/HR2 interaction (*a* and *d* residues) [36] and/or to the presence of an alanine at position 22 (corresponding to position 138 in gp41). An alanine at this position increases the binding affinity of HR2 region to HR1 and enhances the activity of HR2-based HIV-1 fusion inhibitor peptides [47].

The N43K mutation in the HR1 region of HIV-1 was sufficient to confer high-level resistance to this peptide. These results suggest that, like T-20, P3 acts by selectively binding to the HR1 region in the transmembrane glycoprotein of HIV-1. However, P3 potently inhibited the replication of T-20-resistant viruses bearing the V38A and/or the N42D resistance mutations indicating that the pathway of HIV-1 resistance to P3 differs from that of T-20. We were not able to generate HIV-2 isolates resistant to P3 even after 60 days in culture suggesting that the genetic barrier for resistance to P3 might be significantly higher in HIV-2 than in HIV-1.

Peptides with high helical content like P3 tend to be more stable and less susceptible to proteolytic degradation in biological fluids than unstructured peptides like T-20 [7,13]. In addition, they usually display high anti-HIV-1 potency due to an increased binding affinity for HR1 [48,49]. Indeed, we showed that the potent anti-HIV-1 activity of P3 was conserved for at least 3 h. Moreover, P3 bound strongly to a recombinant HIV transmembrane protein. Hence, the high helical content may also contribute to the potent antiviral activity of P3.

Antibodies present in the plasma of HIV-1-infected patients reacted poorly with P3 as compared to T-20. This was expected as HIV-1 and HIV-2 differ significantly in the HR2 region and antibodies naturally generated against this region in HIV-1 patients were unlikely to bind to a peptide derived from HIV-2/SIV. As drug-specific antibodies can compromise the clinical efficacy of therapeutic proteins either by preventing their exposure to the active site or by decreasing their half-life [50], the weaker antigenicity of P3 in HIV-1-infected patients

might translate into a better bioavailability profile and durable clinical efficacy of P3 in HIV-1-infected patients.

Conclusion

In summary, we successfully derived an ancestral peptide (P3) with low antigenicity, high stability, and potent activity against both HIV-1, including variants resistant to T-20, and HIV-2. Our findings provide proof of principle that potent antiviral peptides can be constructed using evolutionary biology strategies. Such strategies should be explored to enhance the production of antiviral peptide drugs, microbicides, and vaccines.

Acknowledgements

The following Research and Institutes of He

[55–57]; pNL4-3 [43], pSG3.1 [58], pHEF-VSVG [59] and pSG3Δenv [52,60] plasmids; T-20-resistant pNL4-3 gp41 (36G) variants [43,44]; T-20 (enfuvirtide) fusion inhibitor; bicyclam JM-2987 (hydrobromide salt of AMD-3100) coreceptor antagonist [61–63]. pROD10 plasmid was a gift from Keith Peden [64].

P.B., A.Q., and N.T. conceived and designed the experiments. P.B., R.C., J.M.M., H.B., P.P., and A.Q. performed the experiments. P.B., A.Q., and N.T. analyzed the data. P.B. and N.T. wrote the article.

Conflicts of interest

This work was supported by grants FCT/SAU-FCT/67673/2006 and PTDC/SAU-FAR/115290/2009 from Fundação para a Ciência e Tecnologia (FCT) (<http://www.fct.pt>), Portugal, and by Collaborative HIV and Anti-HIV Drug Resistance Network (CHAIN) from the European Union. P.B. and R.C. were supported by PhD grants from Fundação para a Ciência e Tecnologia, Portugal. The funders had no role in study design, data collection and analysis, decision to publish, or preparation of the article.

None declared.

References

1. Dando TM, Perry CM. **Enfuvirtide**. *Drugs* 2003; **63**:2755–2766; discussion 2767–2758.
2. Carter NJ, Keating GM. **Maraviroc**. *Drugs* 2007; **67**:2277–2288; discussion 2289–2290.
3. Wild C, Greenwell T, Matthews T. **A synthetic peptide from HIV-1 gp41 is a potent inhibitor of virus-mediated cell-cell fusion**. *AIDS Res Hum Retroviruses* 1993; **9**:1051–1053.

AQ6

In this section please add the following: We thank Luís Oliveira for help in the P3 circular dichroism spectra deconvolution

please change the location of this heading

AQ7

4. Wild CT, Shugars DC, Greenwell TK, McDanal CB, Matthews TJ. **Peptides corresponding to a predictive alpha-helical domain of human immunodeficiency virus type 1 gp41 are potent inhibitors of virus infection.** *Proc Natl Acad Sci U S A* 1994; **91**:9770–9774.
5. Moore JP, Doms RW. **The entry of entry inhibitors: a fusion of science and medicine.** *Proc Natl Acad Sci U S A* 2003; **100**:10598–10602.
6. Liu S, Jing W, Cheung B, Lu H, Sun J, Yan X, *et al.* **HIV gp41 C-terminal heptad repeat contains multifunctional domains. Relation to mechanisms of action of anti-HIV peptides.** *J Biol Chem* 2007; **282**:9612–9620.
7. Eggink D, Berkhout B, Sanders RW. **Inhibition of HIV-1 by fusion inhibitors.** *Curr Pharm Des* 2010; **16**:3716–3728.
8. Mink M, Mosier SM, Janumpalli S, Davison D, Jin L, Melby T, *et al.* **Impact of human immunodeficiency virus type 1 gp41 amino acid substitutions selected during enfuvirtide treatment on gp41 binding and antiviral potency of enfuvirtide in vitro.** *J Virol* 2005; **79**:12447–12454.
9. Johnson VA, Brun-Vezinet F, Clotet B, Gunthard HF, Kuritzkes DR, Pillay D, *et al.* **Update of the drug resistance mutations in HIV-1: December 2009.** *Top HIV Med* 2009; **17**:138–145.
10. Lalezari JP, Henry K, O'Hearn M, Montaner JS, Piliro PJ, Trottier B, *et al.* **Enfuvirtide, an HIV-1 fusion inhibitor, for drug-resistant HIV infection in North and South America.** *N Engl J Med* 2003; **348**:2175–2185.
11. Lazzarin A, Clotet B, Cooper D, Reynes J, Arasteh K, Nelson M, *et al.* **Efficacy of enfuvirtide in patients infected with drug-resistant HIV-1 in Europe and Australia.** *N Engl J Med* 2003; **348**:2186–2195.
12. De Clercq E. **The history of antiretrovirals: key discoveries over the past 25 years.** *Rev Med Virol* 2009; **19**:287–299.
13. Cai L, Jiang S. **Development of peptide and small-molecule HIV-1 fusion inhibitors that target gp41.** *ChemMedChem* 2010; **5**:1813–1824.
14. Eron JJ, Gulick RM, Bartlett JA, Merigan T, Arduino R, Kilby JM, *et al.* **Short-term safety and antiretroviral activity of T-1249, a second-generation fusion inhibitor of HIV.** *J Infect Dis* 2004; **189**:1075–1083.
15. Greenberg ML, Davison DB, Jin L, Mosier S, Melby T, Sista P, *et al.* **In vitro antiviral activity of T-1249, a second generation fusion inhibitor.** *Antiviral Ther* 2002; **7**:S14.
16. Martin-Carbonero L. **Discontinuation of the clinical development of fusion inhibitor T-1249.** *AIDS Rev* 2004; **6**:61.
17. He Y, Xiao Y, Song H, Liang Q, Ju D, Chen X, *et al.* **Design and evaluation of sifuvirtide, a novel HIV-1 fusion inhibitor.** *J Biol Chem* 2008; **283**:11126–11134.
18. Rowland-Jones SL, Whittle HC. **Out of Africa: what can we learn from HIV-2 about protective immunity to HIV-1?** *Nat Immunol* 2007; **8**:329–331.
19. Damond F, Worobey M, Campa P, Farfara I, Colin G, Matheron S, *et al.* **Identification of a highly divergent HIV type 2 and proposal for a change in HIV type 2 classification.** *AIDS Res Hum Retroviruses* 2004; **20**:666–672.
20. Gao F, Yue L, Robertson DL, Hill SC, Hui H, Biggar RJ, *et al.* **Genetic diversity of human immunodeficiency virus type 2: evidence for distinct sequence subtypes with differences in virus biology.** *J Virol* 1994; **68**:7433–7447.
21. de Silva TI, Cotten M, Rowland-Jones SL. **HIV-2: the forgotten AIDS virus.** *Trends Microbiol* 2008; **16**:588–595.
22. Lemey P, Pybus OG, Wang B, Saksena NK, Salemi M, Vandamme AM. **Tracing the origin and history of the HIV-2 epidemic.** *Proc Natl Acad Sci U S A* 2003; **100**:6588–6592.
23. Hu DJ, Dondero TJ, Rayfield MA, George JR, Schochetman G, Jaffe HW, *et al.* **The emerging genetic diversity of HIV. The importance of global surveillance for diagnostics, research, and prevention.** *JAMA* 1996; **275**:210–216.
24. Witvrouw M, Pannecouque C, Switzer WM, Folks TM, De Clercq E, Heneine W. **Susceptibility of HIV-2, SIV and SHIV to various anti-HIV-1 compounds: implications for treatment and postexposure prophylaxis.** *Antivir Ther* 2004; **9**:57–65.
25. Hizi A, Tal R, Shaharabany M, Currens MJ, Boyd MR, Hughes SH, McMahon JB. **Specific inhibition of the reverse transcriptase of human immunodeficiency virus type 1 and the chimeric enzymes of human immunodeficiency virus type 1 and type 2 by nonnucleoside inhibitors.** *Antimicrob Agents Chemother* 1993; **37**:1037–1042.
26. Poveda E, Rodes B, Toro C, Soriano V. **Are fusion inhibitors active against all HIV variants?** *AIDS Res Hum Retroviruses* 2004; **20**:347–348.
27. Borrego P, Calado R, Marcelino JM, Bártolo I, Rocha C, Cavaco-Silva P, *et al.* **Baseline susceptibility of primary human immunodeficiency virus type 2 to entry inhibitors.** *Antivir Ther* 2012; **17**:565–570.
28. Swofford DL. **PAUP*. Phylogenetic analysis using parsimony (*and other Methods). Version 4.** Sinauer-Associates. Sunderland, Massachusetts; 1998.
29. Posada D, Crandall KA. **MODELTEST: testing the model of DNA substitution.** *Bioinformatics* 1998; **14**:817–818.
30. Rodriguez F, Oliver JL, Marin A, Medina JR. **The general stochastic model of nucleotide substitution.** *J Theor Biol* 1990; **142**:485–501.
31. Johnson WC. **Analyzing protein circular dichroism spectra for accurate secondary structures.** *Proteins* 1999; **35**:307–312.
32. Whitmore L, Wallace BA. **DICHROWEB, an online server for protein secondary structure analyses from circular dichroism spectroscopic data.** *Nucleic Acids Res* 2004; **32**:W668–W673.
33. Lobley A, Whitmore L, Wallace BA. **DICHROWEB: an interactive website for the analysis of protein secondary structure from circular dichroism spectra.** *Bioinformatics* 2002; **18**:211–212.
34. Marcelino JM, Barroso H, Goncalves F, Silva SM, Novo C, Gomes P, *et al.* **Use of a new dual-antigen enzyme-linked immunosorbent assay to detect and characterize the human antibody response to the human immunodeficiency virus type 2 envelope gp125 and gp36 glycoproteins.** *J Clin Microbiol* 2006; **44**:607–611.
35. Oliveira M, Brenner BG, Wainberg MA. **Isolation of drug-resistant mutant HIV variants using tissue culture drug selection.** *Methods Mol Biol* 2009; **485**:427–433.
36. Chan DC, Fass D, Berger JM, Kim PS. **Core structure of gp41 from the HIV envelope glycoprotein.** *Cell* 1997; **89**:263–273.
37. Hopp TP, Woods KR. **Prediction of protein antigenic determinants from amino acid sequences.** *Proc Natl Acad Sci U S A* 1981; **78**:3824–3828.
38. Lawless MK, Barney S, Guthrie KI, Bucy TB, Petteway SR Jr, Merutka G. **HIV-1 membrane fusion mechanism: structural studies of the interactions between biologically-active peptides from gp41.** *Biochemistry* 1996; **35**:13697–13708.
39. Sampah ME, Shen L, Jilek BL, Siliciano RF. **Dose-response curve slope is a missing dimension in the analysis of HIV-1 drug resistance.** *Proc Natl Acad Sci U S A* 2011; **108**:7613–7618.
40. Shen L, Peterson S, Sedaghat AR, McMahon MA, Callender M, Zhang H, *et al.* **Dose-response curve slope sets class-specific limits on inhibitory potential of anti-HIV drugs.** *Nat Med* 2008; **14**:762–766.
41. Eggink D, Langedijk JP, Bonvin AM, Deng Y, Lu M, Berkhout B, Sanders RW. **Detailed mechanistic insights into HIV-1 sensitivity to three generations of fusion inhibitors.** *J Biol Chem* 2009; **284**:26941–26950.
42. Champagne K, Shishido A, Root MJ. **Interactions of HIV-1 inhibitory peptide T20 with the gp41 N-HR coiled coil.** *J Biol Chem* 2009; **284**:3619–3627.
43. Adachi A, Gendelman HE, Koenig S, Folks T, Willey R, Rabson A, Martin MA. **Production of acquired immunodeficiency syndrome-associated retrovirus in human and nonhuman cells transfected with an infectious molecular clone.** *J Virol* 1986; **59**:284–291.
44. Rimsky LT, Shugars DC, Matthews TJ. **Determinants of human immunodeficiency virus type 1 resistance to gp41-derived inhibitory peptides.** *J Virol* 1998; **72**:986–993.
45. Cai W, Pei J, Grishin NV. **Reconstruction of ancestral protein sequences and its applications.** *BMC Evol Biol* 2004; **4**:33.
46. Mullins JJ, Nickle DC, Heath L, Rodrigo AG, Learn GH. **Immuno-genetic sequence: the fourth tier of AIDS vaccine design.** *Expert Rev Vaccines* 2004; **3**:S151–S159.
47. Izumi K, Kodama E, Shimura K, Sakagami Y, Watanabe K, Ito S, *et al.* **Design of peptide-based inhibitors for human immunodeficiency virus type 1 strains resistant to T-20.** *J Biol Chem* 2009; **284**:4914–4920.
48. Naito T, Izumi K, Kodama E, Sakagami Y, Kajiwara K, Nishikawa H, *et al.* **SC29EK, a peptide fusion inhibitor with enhanced alpha-helicity, inhibits replication of human immunodeficiency virus type 1 mutants resistant to enfuvirtide.** *Antimicrob Agents Chemother* 2009; **53**:1013–1018.

49. Otaka A, Nakamura M, Nameki D, Kodama E, Uchiyama S, Nakamura S, et al. **Remodeling of gp41-C34 peptide leads to highly effective inhibitors of the fusion of HIV-1 with target cells.** *Angew Chem Int Ed Engl* 2002; **41**:2937–2940.
50. Schellekens H. **Immunogenicity of therapeutic proteins: clinical implications and future prospects.** *Clin Ther* 2002; **24**:1720–1740; discussion 1719.
51. Takeuchi Y, McClure MO, Pizzato M. **Identification of gammaretroviruses constitutively released from cell lines used for human immunodeficiency virus research.** *J Virol* 2008; **82**:12585–12588.
52. Wei X, Decker JM, Liu H, Zhang Z, Arani RB, Kilby JM, et al. **Emergence of resistant human immunodeficiency virus type 1 in patients receiving fusion inhibitor (T-20) monotherapy.** *Antimicrob Agents Chemother* 2002; **46**:1896–1905.
53. Derdeyn CA, Decker JM, Sfakianos JN, Wu X, O'Brien WA, Ratner L, et al. **Sensitivity of human immunodeficiency virus type 1 to the fusion inhibitor T-20 is modulated by coreceptor specificity defined by the V3 loop of gp120.** *J Virol* 2000; **74**:8358–8367.
54. Platt EJ, Wehrly K, Kuhmann SE, Chesebro B, Kabat D. **Effects of CCR5 and CD4 cell surface concentrations on infections by macrophagetropic isolates of human immunodeficiency virus type 1.** *J Virol* 1998; **72**:2855–2864.
55. Foley GE, Lazarus H, Farber S, Uzman BG, Boone BA, McCarthy RE. **Continuous culture of human lymphoblasts from peripheral blood of a child with acute leukemia.** *Cancer* 1965; **18**:522–529.
56. Nara PL, Hatch WC, Dunlop NM, Robey WG, Arthur LO, Gonda MA, Fischinger PJ. **Simple, rapid, quantitative, syncytium-forming microassay for the detection of human immunodeficiency virus neutralizing antibody.** *AIDS Res Hum Retroviruses* 1987; **3**:283–302.
57. Nara PL, Fischinger PJ. **Quantitative infectivity assay for HIV-1 and-2.** *Nature* 1988; **332**:469–470.
58. Ghosh SK, Fultz PN, Keddie E, Saag MS, Sharp PM, Hahn BH, Shaw GM. **A molecular clone of HIV-1 tropic and cytopathic for human and chimpanzee lymphocytes.** *Virology* 1993; **194**:858–864.
59. Chang LJ, Urlacher V, Iwakuma T, Cui Y, Zucali J. **Efficacy and safety analyses of a recombinant human immunodeficiency virus type 1 derived vector system.** *Gene Ther* 1999; **6**:715–728.
60. Wei X, Decker JM, Wang S, Hui H, Kappes JC, Wu X, et al. **Antibody neutralization and escape by HIV-1.** *Nature* 2003; **422**:307–312.
61. De Clercq E, Yamamoto N, Pauwels R, Balzarini J, Witvrouw M, De Vreese K, et al. **Highly potent and selective inhibition of human immunodeficiency virus by the bicyclam derivative JM3100.** *Antimicrob Agents Chemother* 1994; **38**:668–674.
62. Bridger GJ, Skerlj RT, Thornton D, Padmanabhan S, Martellucci SA, Henson GW, et al. **Synthesis and structure-activity relationships of phenylenebis(methylene)-linked bis-tetraaza-macrocycles that inhibit HIV replication. Effects of macrocyclic ring size and substituents on the aromatic linker.** *J Med Chem* 1995; **38**:366–378.
63. Hendrix CW, Flexner C, MacFarland RT, Giandomenico C, Fuchs EJ, Redpath E, et al. **Pharmacokinetics and safety of AMD-3100: a novel antagonist of the CXCR-4 chemokine receptor, in human volunteers.** *Antimicrob Agents Chemother* 2000; **44**:1667–1673.
64. Ryan-Graham MA, Peden KW. **Both virus and host components are important for the manifestation of a Nef- phenotype in HIV-1 and HIV-2.** *Virology* 1995; **213**:158–168.